

EVALUATION OF VEGETATED DUNES FOR EROSION RESISTANCE AGAINST TSUNAMI OVERFLOW

Kunihiro Watanabe¹ and Fuminori Kato¹

A total of 14 soil samples were collected from sand dunes without scattering, and the process of tsunami-induced erosion was observed using hydraulic model experiments. The densities of vegetation roots were measured at 45 points on seven beaches along the Japanese coast. The results of the experiment confirmed that the roots of vegetation highly affected the resistance of soil against erosion. Based on this result, an erosion model based on the index α was proposed, and the relationship between α and root density was described. Then, the applicability of the proposed erosion model was investigated using numerical simulations.

Keywords: tsunami, erosion resistance, sand dune, vegetation, hydraulic model experiment, numerical simulation

1. INTRODUCTION

In the 2011 Great East Japan Earthquake, the number of dead and missing people was just under 20,000, and there was loss and functional damage over a wide area to homes, public facilities, and infrastructure. Most of this damage was caused by the inundation of the tsunami. Based on this experience, the basic design concept of coastal dike height against tsunamis was revised in Japan.

Coastal dikes are designed to prevent the inundation of tsunamis that occur once every few decades or once a century. For more infrequent large tsunamis, such as those induced by the 2011 Great East Japan Earthquake, disaster risk reduction by a combination of structural and non-structural countermeasures should be considered.

Sand dunes and coastal vegetation are expected to function as natural coastal dikes that diminish the tsunami flow. These types of natural features are recognized as green infrastructure or ecosystem-based disaster risk reduction (Eco-DRR). Sand dunes are widely distributed along the Japanese coast, and most dunes were historically reinforced and maintained by local residents. These dunes will prevent inundation of water if the height of the tsunami is lower than the top of the dune. However, if tsunami overflow occurs, the mitigation function may rapidly diminish because of erosion. Although vegetation may increase the resistance of dunes against tsunami over-flow, this effect has not been evaluated.

In this study, we propose a method for estimating the erosion resistance of sand dunes against tsunami over-flow. First, the erosion process of dunes caused by tsunamis was observed using hydraulic model experiments. Based on this result, an erosion model was proposed. Then, the applicability of the proposed erosion model was investigated using numerical simulations.

2. MATERIALS AND METHODS

2.1. Collection of Soil Samples

The compaction of soil and the existence of vegetation roots are expected to affect the erosion caused by the tsunami water flow. Thus, soil samples were collected directly from sand dunes using a square steel frame 1.5 m in length and 0.6m in depth to avoid scattering the soil samples (Fig. 1). The steel frame was inserted in the ground, and the bottom plate was inserted to separate the soil sample from the ground. Roots of vegetation were preserved in the samples using this method.

A total of 14 samples were collected for use in the channel experiment (Table 1).



Figure 1. Collection of soil sample using the steel frame.

¹ National Institute for Land and Infrastructure Management, 1 Asahi, Tsukuba, Ibaraki, 3050804, Japan

Case	Location	Designed Velocity (m/s) and Duration	Evaluation
IZ-1	Izumo, Shimane Pref.	7 m/s : 30 s, 10 s, 10 s, 10 s, 30 s, 60 s	Eq. 1
IZ-2	Izumo, Shimane Pref.	7 m/s : 1 min 20 s, 1 min 20 s	Eq. 1
IZ-3	Izumo, Shimane Pref.	7 m/s : 10 s, 30 s, 10 s, 10 s, 10 s, 10 s	Eq. 1
IW-1	Iwanuma, Miyagi Pref.	1m/s : 35 min, 2 m/s : 5 min, 1 min, 3m/s : 1 min, 1 min, 1 min, 4 m/s : 1 min, 1 min	-
IW-2	Iwanuma, Miyagi Pref.	1m/s : 30 min, 2 m/s : 1 min, 1 min, 3m/s : 1 min, 1 min, 1 min, 4 m/s : 1 min, 1 min, 1 s	-
F-1	Fukuroi, Shizuoka Pref.	1 m/s : 29 min 20 s, 7 m/s : 1 s, 1 s, 1 s, 1 s, 1 s, 2 min, 3 min	Eq. 1
F-2	Fukuroi, Shizuoka Pref.	1 m/s : 25 min, 7 m/s : 1 s, 1 s, 1 s, 1 s	Eq. 1
F-3	Fukuroi, Shizuoka Pref.	1 m/s : 20 min, 7 m/s : 1 s, 1 s, 1 s, 1 s	Eq. 1, Eq. 2
F-4	Fukuroi, Shizuoka Pref.	1 m/s : 25 min, 7 m/s : 1 s	Eq. 1, Eq. 2
S-1	Shirako Chiba Pref.	1 m/s : 1 min 25 s, 3 min, 36 min, 7 m/s : 1 s, 1 s, 30 s, 1 min, 1 min, 2 min, 18 min, 20 min	Eq. 1
S-2	Shirako Chiba Pref.	1 m/s : 25 min, 7 m/s : 1 min, 1 s, 10 s, 1 s, 1 s, 1 s, 10 s	Eq. 1
IS-1	Ishikarihama, Hokkaido Pref.	1 m/s : 19 min, 3 m/s : 1 s, 1 s, 5 m/s : 1 s, 1 s, 7 m/s : 1 s	Eq. 1, Eq. 2
IS-2	Ishikarihama, Hokkaido Pref.	1 m/s : 20 min, 3 m/s : 1 min, 3 min, 5 min, 5 m/s : 30 s, 3 min, 10 min, 7 m/s : 1 min, 10 min	Eq. 1, Eq. 2
IS-3	Ishikarihama, Hokkaido Pref.	1 m/s : 22 min, 3 m/s : 1 min, 5 min, 1 min, 5 m/s : 1 min, 3 min, 1 min, 7 m/s : 1 min, 10 min	Eq. 1, Eq. 2

2.2. Vegetation Survey

Species distribution of vegetation and plants was surveyed near the collected soil sample and seven coasts around Japan (Table 2). The density of vegetation roots and the particle size of the soil were measured at 45 points on these coasts. These coasts were selected to include a variety of different environments, and the survey points were located between the sandy beach and the sand dunes behind it. At Iwanuma Beach, the artificial soil mound formed on the landward slope of the coastal embankment was selected.

The soil and vegetation roots were collected every 3–10 cm in depth on a square quadrat with side length of 50 cm; then, the depth distribution of roots and the particle size were measured. The collected roots were categorized into five stages based on the thickness, and the weight of the entirety of the roots was measured for each category. The root densities were calculated for each layer by dividing the total root weight by the total volume of each layer.

Survey Site	Location	
Ishikarihama	Ishikari, Hokkaido Pref.	Japan Sea Side, Subarctic Zone
Iwanuma Beach	Iwanuma, Miyagi Pref.	Bare Ground, Test Planting Area
Ichinomiyamachi Hakui	Jike Town, Hakui, Ishikawa Pref.	Japan Sea Side
Fukuroi	Nakashinden, Fukuroi, Shizuoka Pref.	Pacific Ocean Side
Geisei Beach	Geisei Village, Aki-gun, Kochi Pref.	Pacific Ocean Side
Miyazaki Beach	Horinouchi, Takanabe, Miyazaki Pref.	Pacific Ocean Side
Toguchinohama	Irabu, Miyakojima, Okinawa Pref.	Subtropical Marine Climate Zone

2.3. Experimental Channel

The experimental channel was an open channel 8.9 m in length and 1.2 m wide, with a gradient of 1/250 (Fig. 2). Soil samples were placed in the center of the channel and adjusted so that the bottom of the channel and the surface of the sample were located at the same height.

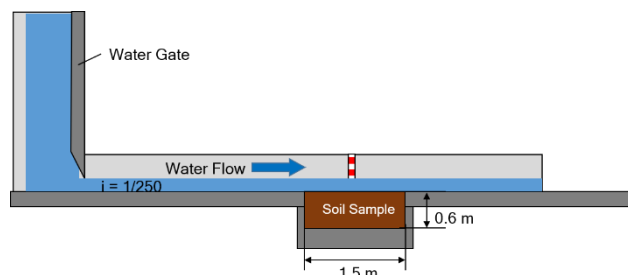


Figure 2. Side view of the experimental channel.

2.4. Exposure to water flow

The samples were exposed to high-velocity flows, imitating tsunami overflow. Changes in the depth of the surface were measured. The flow velocity was gradually increased to the proposed value. The flow velocity was maintained for the proposed duration after reaching the target speed, after which the water flow was stopped and the depth of erosions was measured. Fig. 3 shows an example of the time series change in water velocity for case IZ-3. In this case, the proposed velocity was 7 m/s, and exposure to this velocity of water was repeated six times. The soil samples were exposed to a 1-m/s water flow before starting the above procedure, to decrease the air contained in the samples. The proposed velocities and durations of water flow are shown in Table 1 for each case.

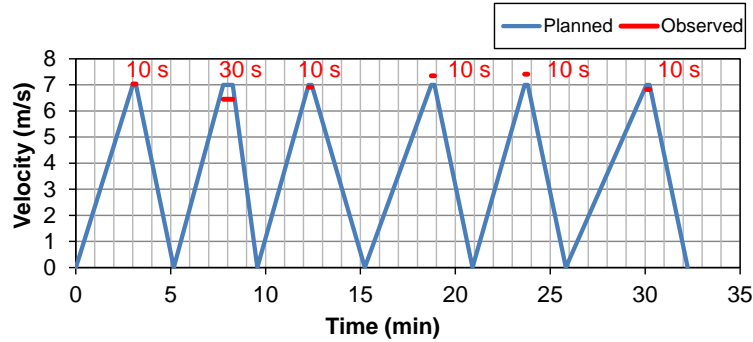


Figure 3. Time series change in water velocity and duration for case IZ-3

During the experiment, if the height of the soil surface decreased below the surface of the channel floor, the sample was raised to the height of the channel floor and exposed to water flow again. The depth of erosion was measured on a 10-cm-interval grid, and the average erosion depth was calculated using all data except that measured 10 cm from the left and right sides and 20 cm from the upper and lower sides. Localized scouring resulting from the side walls and steel frame was observed.

The flow velocity was measured using pitot tubes; the relationship between the flow speed and water level of the reservoir tank was estimated previously. Based on this relationship, the flow velocity was controlled by monitoring the water level of the reservoir tank during the experiment. A tiny colored float was added to the water flow and recorded by a high-speed camera. The flow velocity was determined by analyzing the movement of this float after the experiment.

2.5. Evaluation of resistance to erosion

The index α representing the resistance to soil erosion was introduced. This index was proposed by Uda et al. (1997) to consider the effect of vegetation when calculating the erosion on the surface of a river bank. In this study, this index was simplified as described below. A lower value of α means that soil has a higher resistance to erosion.

$$z = \alpha u_* \log t \quad (1)$$

where z is the erosion depth (cm), α is a constant representing the erosion resistance of the root system, u_* is the friction velocity (m/s), and t is the time of exposure to water flow (min).

This equation can be applied where the friction velocity does not change over time. For conditions where the friction velocity varies over time, Uda et al. (1997) also proposed the following equation to calculate the depth of erosion per unit time (hereinafter, erosion rate):

$$\frac{dz}{dt} = \frac{\alpha u_*}{\ln 10} \exp\left(-\frac{\ln 10}{\alpha u_*} z\right) \quad (2)$$

The friction velocities were estimated using the Manning formula (Eq. 3) assuming uniform flow.

$$u_* = \sqrt{gn^2 v^2 h^{-1/3}} \quad (3)$$

where n is the roughness coefficient (0.03 was used in this study), v is the average cross-sectional velocity, and h is the water depth.

The proposed water velocities and the observed water depth were applied to Eq. 3 when estimating the index alpha based on Eq. 1. The observed water velocities were applied to Eq. 3 when using Eq. 2.

The time series change in the depth of erosion was calculated assuming multiple candidates for index α , and index α was determined by comparing the estimated change with the observed change. Before carrying out this process, we searched for points at which the erosion depth increased significantly, and the time series data observed before that point were used for comparison.

2.6. Numerical Simulation

Topographical changes induced by the 2011 Tohoku Tsunami were investigated on the Kujukuri coast in Japan. The eroded sand dunes were searched by eye, comparing aerial photographs taken after the tsunami with photographs taken before the disaster. The changes in elevation were estimated from data obtained by the aviation laser survey conducted after the 2011 Tohoku Tsunami.

Tsunami run-up simulation was conducted on the same area to investigate the applicability of the evaluation of erosion resistance defined based on the experiments. Tsunami run-up was calculated using non-linear long wave theory with consideration of friction at the sea floor and an advection term. The equation of continuity (Eq. 4) and the equation of motion (Eq. 5 and Eq. 6) are described below (Imamura et al. 2006).

$$\frac{\partial \eta}{\partial t} + \frac{\partial M}{\partial x} + \frac{\partial N}{\partial y} = 0 \quad (4)$$

$$\frac{\partial M}{\partial t} + \frac{\partial}{\partial x} \left(\frac{M^2}{D} \right) + \frac{\partial}{\partial y} \left(\frac{MN}{D} \right) + gD \frac{\partial \eta}{\partial x} + \frac{gn^2}{D^{7/3}} M \sqrt{M^2 + N^2} = 0 \quad (5)$$

$$\frac{\partial N}{\partial t} + \frac{\partial}{\partial x} \left(\frac{MN}{D} \right) + \frac{\partial}{\partial y} \left(\frac{N^2}{D} \right) + gD \frac{\partial \eta}{\partial y} + \frac{gn^2}{D^{7/3}} N \sqrt{M^2 + N^2} = 0 \quad (6)$$

where D is the total water depth given by $h + \eta$, M and N are the discharge flux in the x- and y- directions which are given by Eq. 7, and Eq. 8. n is Manning's roughness.

$$M = u(h + \eta) = uD \quad (7)$$

$$N = v(h + \eta) = vD \quad (8)$$

where u and v are the average velocities in x- and y- directions.

The change in topography was simulated by calculating the bed load layer and the suspended sand layer following Takahashi et al. (2011). The amounts of bed load and suspended sand lifted and settled were calculated for each grid, and the topographical change was calculated by solving the continuous equations for the bed load and suspended sand layers.

The erosion of the sand dune was simulated in two phases. Until the erosion depth reached 2 cm, the change in depth was calculated based on Eq. 2, considering the effect of vegetation, and Eq. 9 was used to calculate erosion depth exceeding 2 cm. The effect of the roundness of the bank on erosion was considered using the correction factor (Eq. 10) following Fujisawa et al. (2011) because it is possible for the convex shape of the bank to promote erosion.

The results of the sand dune erosion calculation were reflected in the terrain data used for the calculation of tsunami run-up.

$$\frac{dz}{dt} = \gamma u_* \quad (9)$$

where u_* is friction velocity estimated by Eq. 3, and γ is coefficient of resistance to erosion for cray.

$$z_\beta = 0.5z \left\{ \exp \left(-\beta \frac{\partial^2 h}{\partial x^2} \right) + \exp \left(-\beta \frac{\partial^2 h}{\partial y^2} \right) \right\} \quad (10)$$

where z_β is corrected depth of erosion, h is elevation, and β is correction coefficient for roundness in shape.

3. RESULTS

3.1. Hydraulic model experiment

The depths of erosion varied among the 10-cm grid, because it was prevented by roots and gravel; thus, the average depth of erosion was analyzed in this study. Fig. 4. shows a representative result observed for Case IZ-3. In this case, the surface of the soil sample was eroded gradually, but the speed of erosion was slow during the first 15 min (after being exposed to 7 m/s water flow three times). Most amount of soil was flushed out and the roots of tree were exposed (Fig. 5). However, the erosion speed was rapidly increased after the depth of erosion reached 10 cm.

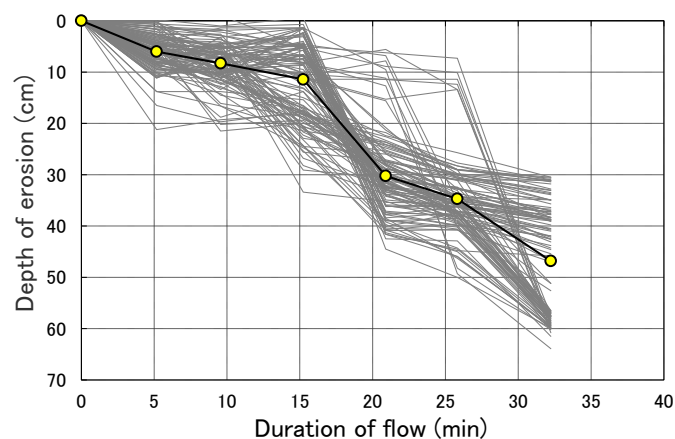


Figure 4. Change in the depth of erosion throughout the experiment (Case IZ-3). Gray lines represent the depth measured for each grid, and the black line with circle markers is the average depth.

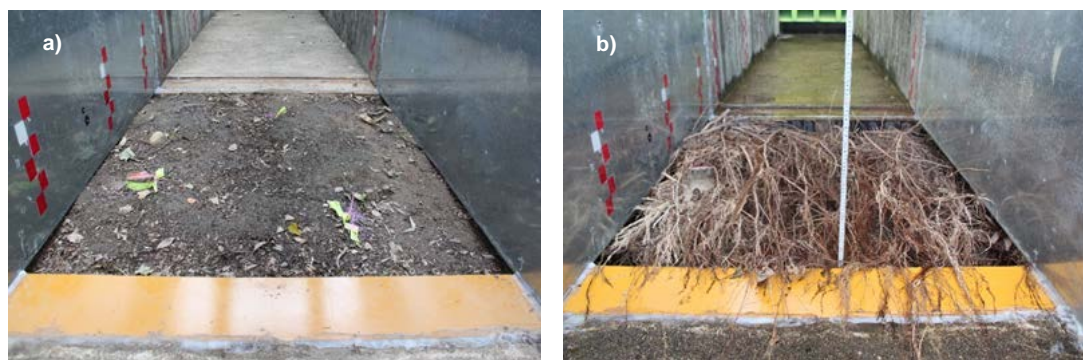


Figure 5. Surface of the soil sample before the experiment (a) and after being exposed to 7 m/s water flow three times(b) (Case IZ-3).

Fig. 6. a). shows another representative result observed for Case F-3. In this case, the proposed velocity of water flow began at 1 m/s for approximately 30 min, before being changed 7 m/s. However, the observed velocity reached 9 m/s when the intended velocity was 7 m/s. The surface of the sample was covered with grass before exposure to water flow (Fig. 7). The average depth of erosion reached 4 cm, and the surface of the sample was covered by exposed long grass after being exposed to 1 m/s water flow. Following this, the average erosion depth accelerated rapidly when water flowed at a velocity of 9 m/s, but the surface of the sample remained covered in grass until the end of the experiment.

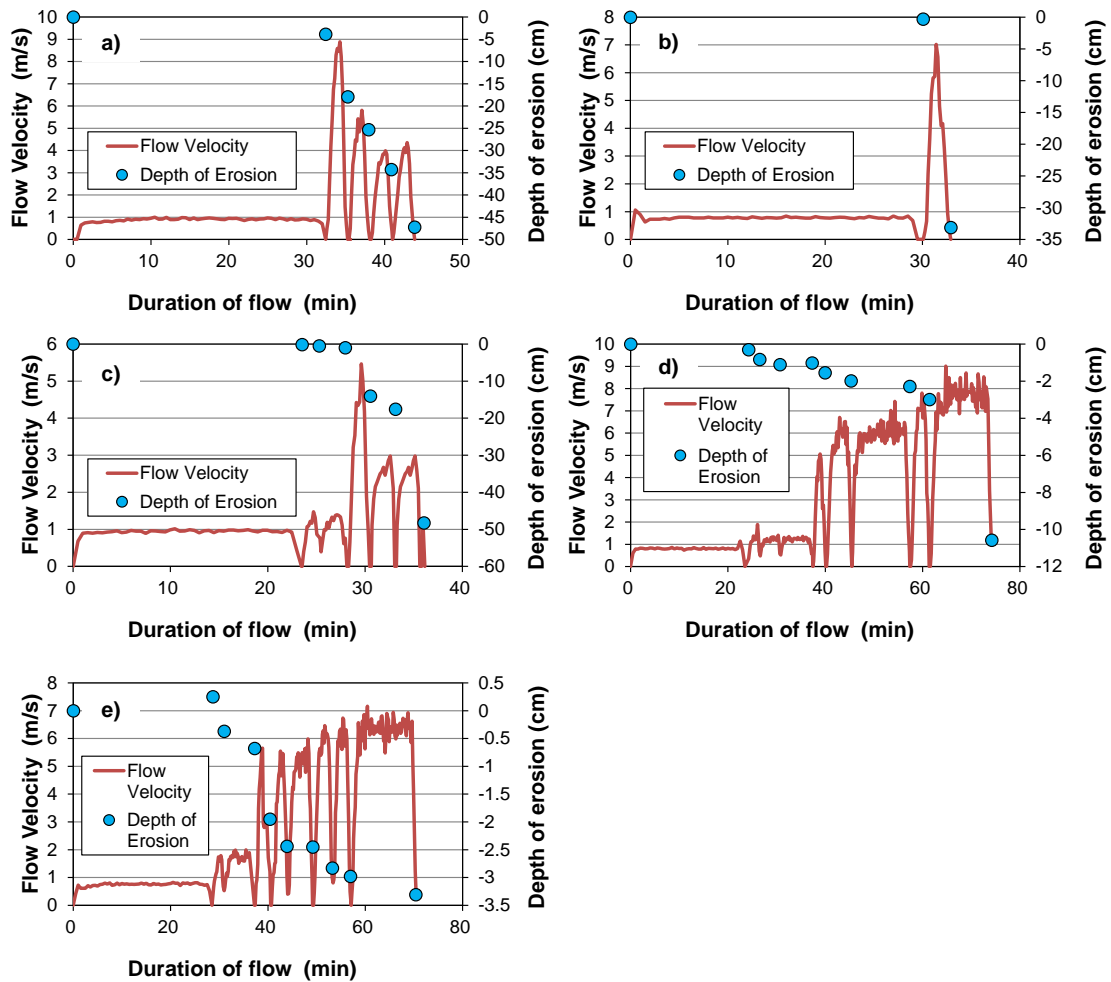


Figure 6. Change in the flow velocity and the depth of erosion throughout the experiment; a) Case F-3, b) Case F-4, c) Case IS-1, d) Case IS-2, e) Case IS-3.

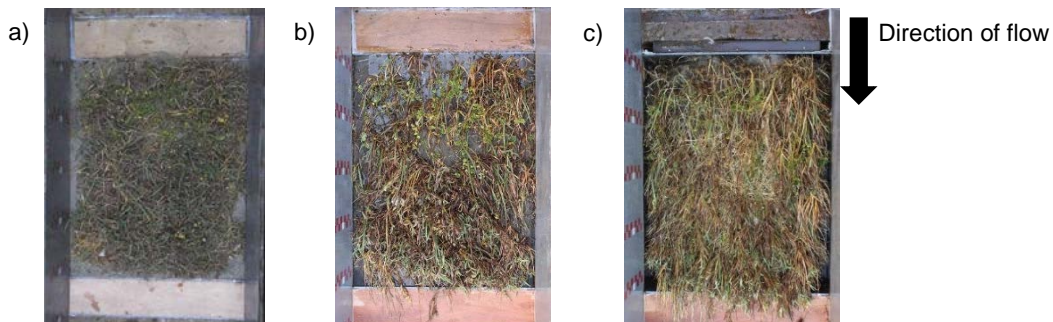


Figure 7. Surface of the soil sample before the experiment (a), after being exposed to 1 m/s water flow (b), and after being exposed to 9 m/s water flow (c) (Case F-1).

3.2. Distribution of root density on the coasts

The density of vegetation roots was comparatively high on Ishikarihama. The root density was high at a certain depth below the ground surface and tended to decline in deeper layers. This tendency was also observed for approximately half of the 45 locations surveyed, and a relatively large number of roots was observed in layers up to 10 cm from the surface of the ground (Fig. 8). When focusing on fine roots, defined as the roots with diameters of 5 mm or less, the root density was generally near 0.01 g/cm^3 , with a range up to 0.06 g/cm^3 distributed among 43 locations (Fig. 9).

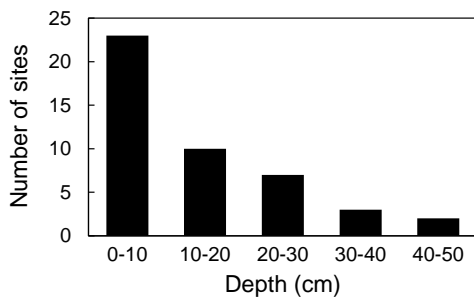


Figure 8. Distribution of the depth where the highest root density was observed.

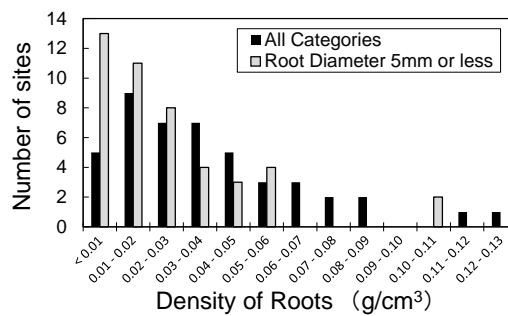


Figure 9. Distribution of the highest root density observed for each site.

3.3. Erosion resistance against water flow

Fig. 10 shows the relationship between the index α and the fine root density. Both estimations of the index α , based on Eq. 1 and Eq. 2, are shown. The dotted line ($\alpha = -50 \sigma + 9$) represents the upper limits for the index α that was described by Uda et al. (1997) for vegetation growing on river embankment slopes. The index α was higher than the upper limit at a fine root density of less than 0.01 g/cm³, and lower at a fine root density of 0.01 g/cm³ or higher. The index α determined based on Eq. 1 tended to be smaller than the value determined using Eq. 2.

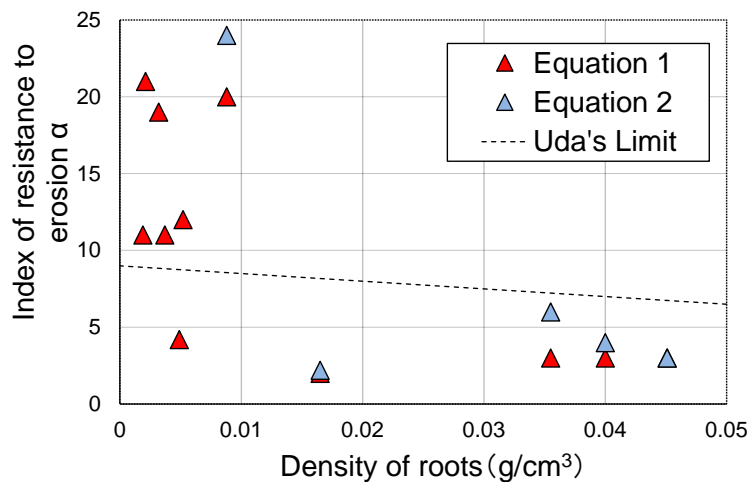


Figure 10. Relationship between root density and resistance to erosion estimated based on the results of channel experiment.

3.4. Numerical Simulation

Two types of erosion were observed at the Kujukuri coast. One type was suspected to be formed by the water flow of the tsunami that overtopped and flowed down the land side of the sand bank (Fig. 11). Another type was formed by a tsunami flowing through where the height of the sand bank was partially low. The heights of the sand banks were approximately 6 m above the Tokyo pail (mean water level on the Tokyo port), and the height of the tsunami was estimated to be 2 – 3 m above the top of the sand bank. In this area, the sand bank was located behind the sea wall, and the bank was entirely covered by vegetation (Fig. 12). The analysis by the aviation laser survey showed that the decrease in elevation was approximately 2 m on the most eroded part.

The result of the simulation matched closely with the height change observed at the site (Fig. 13).



Figure 11. Erosion on sand bank (a) before the tsunami (16. Oct. 2009) and (b) after the 2011 Tohoku Tsunami (31. Mar. 2011).



Figure 12. Sand bank analyzed in this study.

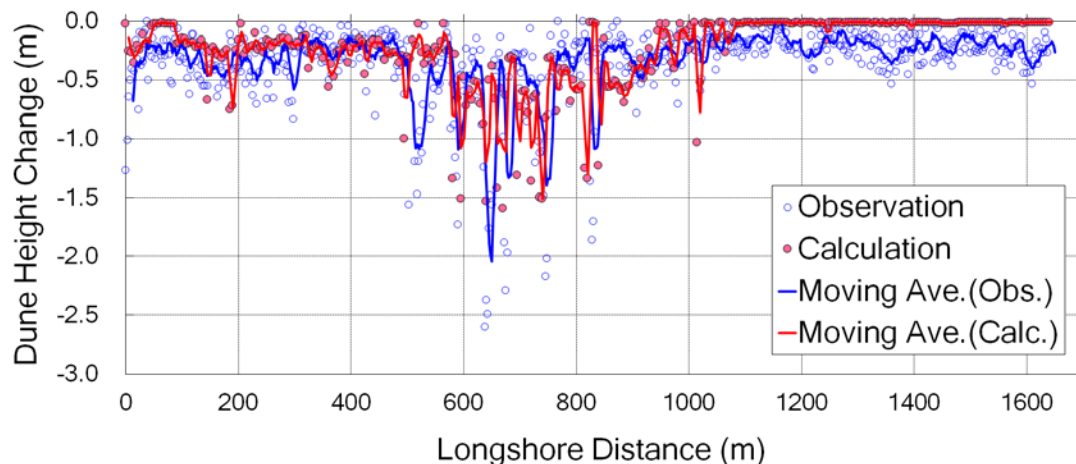


Figure 13. Observed and numerically estimated height change in sand bank located on the Kujukuri Coast, Chiba Prefecture, Japan.

4. DISCUSSION

4.1. Erosion Process in Surface Layer of Sand Dunes

The results of the hydraulic model experiment suggest that the depth of erosion caused by water flow increased relatively slowly to the depth at which the roots of the vegetation were densely distributed. However, the erosion speed tended to increase rapidly after the depth of erosion exceeded that depth. Based on these results, the depth at which the vegetation root system is densely distributed can be defined as the erosion limit. The erosion resistance of the root system should be considered until the depth of erosion reaches the erosion limit when estimating the tsunami run-up considering the tsunami-induced topographic change, and the continuous sediment transport equation should be used after the erosion limit is reached (Fig. 14).

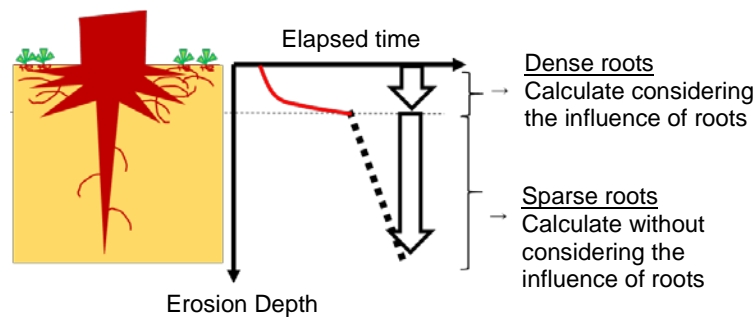


Figure 14. Principles for calculating the erosion process on sand dune with vegetation in the surface layer.

4.2. Erosion Resistance and Root Density

The estimated index α was higher than the upper limit proposed by Uda et al. (1997) at a fine root density of less than 0.01 g/cm^3 , and lower at a fine root density of 0.01 g/cm^3 or higher. Considering that Uda et al. (1997) obtained their upper limit mostly for fine root densities of 0.02 to 0.08 g/cm^3 , the α value estimated by our experiment for a fine root density of 0.01 g/cm^3 or greater was consistent with Uda et al. (1997).

However, the range of the surveyed depth for each layer was wider than that measured by Uda et al. (1997). The fine root density in the surface layer may be larger if the root density were measured for the same layer thickness as measured in Uda et al. (1997). Uda's upper limit should be used as the index α when the erosion of sand dunes is simulated for disaster prevention.

The index α was estimated based on both Eq. 1 and Eq. 2 for the five cases, and the results showed that the index α was smaller if Eq. 1 was used. Because of the limitation of the obtained data, the index α was estimated based only on Eq. 1 for a fine root density of less than 0.01 g/cm^3 in this study. It should be kept in mind that the index α may be overestimated for a fine root density of less than 0.01 g/cm^3 .

4.3. Tsunami Run-up Simulation Considering the Erosion Resistance of Sand Dune

The results of the simulation matched closely with the height change observed at the site. This suggests that the root density of vegetation affected the degree of dune erosion caused by the 2011 Tohoku Tsunami, and also suggests that the topographical change in the sand dune would be predictable by considering the index α . However, only one site was investigated in this study; a precise method for simulation should be developed by conducting the same study on many sites.

In the planar two-dimensional nonlinear long wave theory, the velocity in the vertical direction is set at 0, and the velocity in the horizontal direction is the average cross-sectional velocity. It is also necessary to keep in mind that tsunami-induced vortexes formed on the rear vertical walls cannot be expressed, and the accuracy of the velocity and run-up height may be low in area with large gradients. Where the gradient of the land side slope of sand dunes is steep, long wave theory is not able to sufficiently model the tsunami flow on the land side slope.

For more efficient calculations, sand dunes are treated as calculation grid structures rather than ground in the calculation, and they may be processed such that the sand dune disappears at the point at which the sand dune erosion reaches the erosion limit.

The above-ground portions of trees, such as trunks, also have the effect of dissipating the flow of a tsunami, and many studies related to this concept have been conducted. These effects should be considered simultaneously in the tsunami run-up simulation.

5. CONCLUSIONS

The main conclusions of this study are as follows.

- Vegetation surveys conducted on seven beaches showed that the roots of vegetation tended to be distributed with relatively high density from the surface to 10 cm below the sand dune.
- The process of tsunami-induced erosion on the sand dune was observed with a channel experiment, and it was confirmed that the roots of vegetation significantly affect the resistance of soil against erosion.
- The parameter α , which reflects the erosion resistance of the soil, was estimated based on the results of the channel experiment, and the relationship between α and root density was described. This made it possible to evaluate the erosion resistance of ground with vegetation using the root density.

ACKNOWLEDGMENTS

In the survey of Ishikarihama, Dr. Hajime Matsushima of the Hokkaido University Research Faculty of Agriculture provided valuable advice. The calculation of topographical changes was led by Dr. Kei Yamashita of the Tokyo University International Research Institute of Disaster Science. In the collection of research information, valuable advice was received from the National Agriculture and Food Research Organization Institute of Agrobiological Sciences Water Resources Engineering and Coastal Hydraulics Unit and the Forest Research and Management Organization Forest Research Department of Disaster Prevention, Meteorology and Hydrology. Cooperation was received in the collection of samples from various locations from the Ministry of Agriculture, Forestry and Fisheries Ishikari Forest Management Office, the Hokkaido Government, Ishikari City Hall, Ishikari Bay New Port Authority, Shizuoka Prefectural Office, Shizuoka Prefecture Fukuroi Public Work Office and Shizuoka Chuen Agriculture and Forest Bureau. Permission was also obtained from local administrators in the field survey of vegetation. In the summarizing of research results, valuable advice was received from the Shizuoka Prefecture Transport and Infrastructure Department and Emergency Management Department. We would like to take this opportunity to express our thanks. And we also would like to thank Editage (www.editage.com) for English language editing.

REFERENCES

- Fujii, N., M. Ikeno, T. Sakakiyama, M. Matsuyama, M. Takao and Ken Mukohara. 2009. Hydraulic Experiment on Flow and Topography Change in Harbor due to Tsunami and Its Numerical Simulation, *Journal of JSCE B2 (Coastal Engineering Committee)*, Vol.65, No.1, 291-295. (in Japanese)
- Imamura, F., A. C. Yalciner and G. Ozyurt. 2006. Tsunami modeling manual(TUNAMI model). <http://www.tsunami.civil.tohoku.ac.jp/hokusai3/J/projects/manual-ver-3.1.pdf>
- Takahashi, T., T. Kurokawa, M. Fujita and H. Shimada. 2011. Hydraulic Experiment on Sediment Transport due to Tsunamis with Various Sand Grain Size, *Journal of JSCE B2 (Coastal Engineering Committee)*, Vol. 67, No. 2, I_231-I_235. (in Japanese)
- Uda, T., T. Mochizuki, K. Fujita, K. Hirabayashi, K. Sasaki, A. Hattori, M. Fujii, W. Fukaya and O. Tairadate: Behavior of Multiple Natural River Embankments, Viscous Soil and Vegetation under Flood Flows, Public Works Research Institute Papers, Vol. 3489, pp.97-214, 1997. (in Japanese)